Tunable Nonadiabatic Excitation in a Single-Electron Quantum Dot

M. Kataoka,[1] J. D. Fletcher,[1] P. See,[1] S. P. Giblin,[1] T. J. B. M. Janssen,[1] J. P. Griffiths,[2] G. A. C. Jones,[2] I. Farrer,[2] and D. A. Ritchie[2]

[1]*National Physical Laboratory, Hampton Road, Teddington, Middlesex TW11 0LW, United Kingdom*
[2]*Cavendish Laboratory, J J Thomson Avenue, Cambridge CB3 0HE, United Kingdom*

(Received 14 December 2010; published 21 March 2011)

We report the observation of nonadiabatic excitations of single electrons in a quantum dot. Using a tunable-barrier single-electron pump, we have developed a way of reading out the excitation spectrum and level population of the dot by using the pump current as a probe. When the potential well is deformed at subnanosecond time scales, electrons are excited to higher levels. In the presence of a perpendicular magnetic field, the excited states follow a Fock-Darwin spectrum. Our experiments provide a simple model system to study nonadiabatic processes of quantum particles.

DOI: 10.1103/PhysRevLett.106.126801 PACS numbers: 73.23.Hk, 73.63.Kv

Just as the surface of water ripples when a glass is moved, motion of quantum particles can be induced by a sudden change in their environment. A simple example is a particle confined in a potential well whose shape varies in time [1]. If the change is slow compared to the motion of the particle, the particle adiabatically follows the same quantum state. If the change is too fast, the particle can be found in a superposition of states. This concept of nonadiabaticity is at the heart of quantum dynamic processes [2], and understanding it is of great importance in developing quantum technologies, e.g., controlling chemical reactions between molecules [3,4] or manipulating coherent single-particle states [5–11]. There are, however, few experimental systems that demonstrate nonadiabatic transitions in a tunable way.

In this Letter, we report the observation of nonadiabatic excitations in a very simple model system—a single electron trapped in a quantum dot [12,13]. Rapid modulation of the confinement potential causes transitions to excited orbital states. The resulting occupation probabilities are measured by selectively letting the electrons in each state escape to a reservoir. We investigate the effect of the rate of potential modulation on the transition probabilities and confirm that the excitations are due to the potential deformation rather than thermal or resonant effects. Our results show the crossover from the adiabatic to the nonadiabatic regime, demonstrating the fragility of quantum states subject to rapid perturbation of their environment.

We realize a dynamic single-electron system based on a tunable-barrier quantum-dot pump [14,15] [Fig. 1(a)]. Negative voltages V_{G1} and V_{G2} applied to the two finger gates ($G1$ and $G2$) define a quantum dot in the region between them. An ac voltage V_{rf} added to $G1$ captures electrons from the source reservoir into the dot and pumps them out into the drain reservoir, generating a dc current between the two reservoirs. The relation between the cycle in V_{rf} and the changes in the electrostatic confinement potential is shown in Figs. 1(b) and 1(c). As the barrier potential defined by $G1$ progressively rises, (i) electrons are trapped into the dot, (ii) excess electrons tunnel back to the original reservoir (source) as they are lifted above the Fermi energy E_{F}, and (iii) the remaining electrons are trapped in the dot and (iv) are ejected into the drain electrode, generating an electric current. The critical part of the pump operation is phase (ii) when the last excess electron tunnels back to the source [16]. If this escape probability is unity, and if the escape probability is zero for the rest of the electrons in the dot, then the current is quantized at $I = Nef$, where N is the number of electrons pumped per cycle, e is the elementary charge, and f is the frequency of V_{rf}. N can be tuned by adjusting V_{G2}, which changes the size of the dot (and hence the electron energy levels). For $N = 1$ and $f = 1$ GHz, $I = 160$ pA [17]. Although one complete pump cycle lasts $\sim$1 ns (for $f \sim 1$ GHz), the measured current is determined by the tunneling processes during a small fraction of the cycle in phase (ii). It is this sensitivity which enables the pump current to probe nonadiabatic processes taking place on picosecond time scales, providing information about the excitation spectrum and level population of the dot.

During a pump cycle, if the rate of confinement potential modulation is sufficiently slow, the electron is likely to stay in the ground state of the dot, as shown in Fig. 1(d). For fast enough modulation, nonadiabatic transitions to excited states occur [1]. When the excited state has a large enough tunnel rate Γ_{ES} to the reservoir (the tunnel rate of the ground state Γ_{GS} is in general weaker than that of excited states, i.e., $\Gamma_{\mathrm{ES}} > \Gamma_{\mathrm{GS}}$), the electron will tunnel back to the source reservoir [Fig. 1(e)]. As a result, in this nonadiabatic case, the pump current becomes lower than ef. This way we detect the nonadiabatic excitation, and its transition probability is estimated from the reduction in current.

The samples were fabricated on a GaAs/AlGaAs heterostructure with a two-dimensional electron gas 70 nm below the surface. The two-dimensional electron gas density measured at 1.5 K was 2.7×10^{15} m^{-2}, and the electron mobility was 70 m^2/V s. A 2 μm wide channel

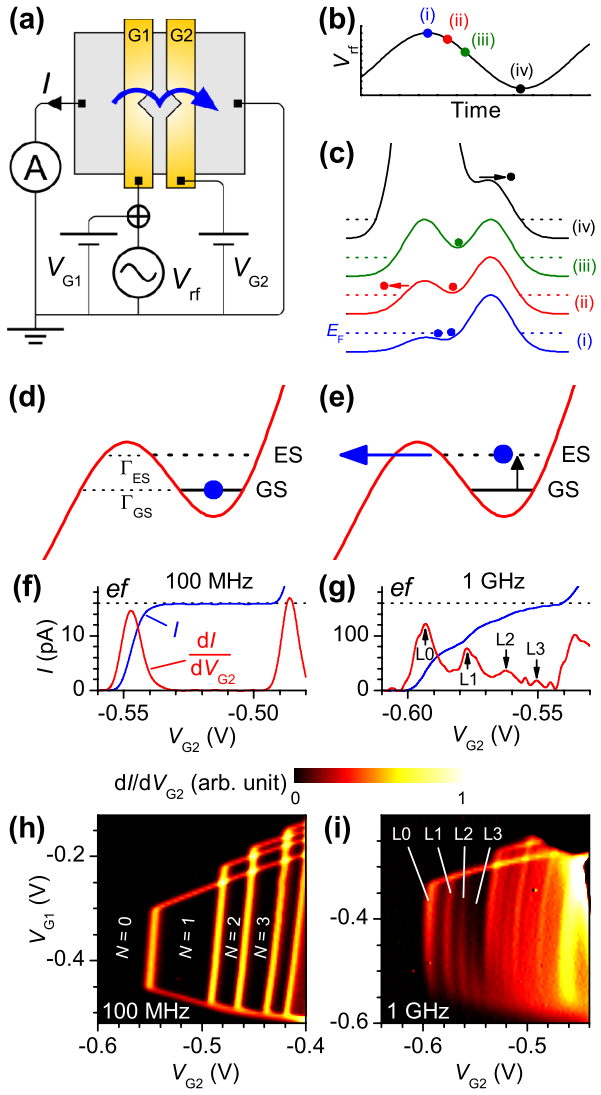

FIG. 1 (color online). (a) Schematic of the single-electron pump device and experimental circuit. (b),(c) The relation between the applied rf signal (V_{rf}) and the electrostatic confinement potential at different parts of the cycle. (d),(e) Close-up of the confinement potential for step (ii) in (c) for cases of adiabatic (d) and nonadiabatic (e) changes in the potential. (f),(g) Pump current I and dI/dV_{G2} as a function of V_{G2}, taken with $B = 6$ T and $f = 100$ MHz (f) and 1 GHz (g). (h),(i) dI/dV_{G2} as V_{G1} and V_{G2} are varied, taken with $f = 100$ MHz and 1 GHz, respectively, at $B = 6$ T.

was defined by etching the surface by ~40 nm. This is in contrast to previous studies [14,15], where narrower (500 nm–1 μm) channels were used. While in the samples of Refs. [14,15] the confinement potential transverse to the transport direction is given by channel etching, in ours the confinement potential is defined by the gate shape [Fig. 1(a)]. Two gates were patterned by using electron-beam lithography, depositing 10/40 nm Ti/Au. The measurements were performed at 300 mK. The rf signal was added onto V_{G1} through a 6 dB attenuator [18], and the current was measured by an ammeter.

Figure 1(f) shows the pump current I and its derivative dI/dV_{G2} (which highlights the transitions between regions of constant current) taken at $f = 100$ MHz in a perpendicular magnetic field $B = 6$ T. Here, a current plateau appears at the quantized value of ef (~ 16 pA), showing that one electron is pumped per cycle. When the frequency is increased to 1 GHz [Fig. 1(g)], the plateau becomes sloped, as well as showing a series of miniature plateaux, separated by the peaks in the derivative marked as $L0$, $L1$, $L2$, and $L3$. The $L0$ peak represents the first rising edge of the current and corresponds to the $N = 0$ to $N = 1$ transition observed at 100 MHz [Fig. 1(f)]. We argue that peaks $L1$, $L2$, and $L3$ appear because the electron is excited nonadiabatically into the first, second, and third excited states, respectively. In the miniature plateau region between $L0$ and $L1$, all the excited states are strongly coupled to the source reservoir, and hence electrons excited into one of these states escape from the dot. Only the electrons that stay in the ground state are pumped from source to drain, and hence the current is reduced to a fraction of ef. As V_{G2} is made more positive, crossing the $L1$ peak means that the tunnel rate of the first excited state becomes small enough that the electron in this state stays in the dot and is pumped, contributing to the overall current. The miniature plateau appears because the probability of keeping the electrons in the first excited state becomes unity and does not change within a small change in V_{G2}. The same argument applies to the $L2$ and $L3$ peaks. In Figs. 1(h) and 1(i), we show the derivative of pumped current as V_{G1} and V_{G2} are varied, taken with $f = 100$ MHz and 1 GHz, respectively, at $B = 6$ T. Here, dI/dV_{G2} is plotted in a color scale. For the $f = 100$ MHz case [Fig. 1(h)], quantized current plateaux appear in the regions marked $N = 1, 2, 3, \ldots$. However, for $f = 1$ GHz, vertical stripes appear in the $N = 1$ region, again marked $L1$, $L2$, and $L3$, which correspond to peaks in dI/dV_{G2} [Fig. 1(i)]. We now study in detail the magnetic-field and frequency dependences of these lines and conclude that these features are indeed due to nonadiabatic excitations.

Figures 2(a) and 2(b) show dI/dV_{G2} for $f = 100$ MHz and 1 GHz, respectively, taken at a fixed V_{G1} in a range of B. The 100 MHz data show no signature of excitation lines, while the 1 GHz data show how the excitation spectrum evolves as a function of B. In Fig. 2(c), the data in Fig. 2(b) are replotted so that the positions of the excitation lines are referenced to the position of the $L0$ line. The distance to the $L0$ line is indicative of the excitation energy of each state. These match well to the Fock-Darwin spectrum observed in few-electron quantum dots [12,13]. The energy states of a two-dimensional circular dot in a perpendicular magnetic field are $E(n, l) = (2n + |l| + 1)\hbar\sqrt{\omega_0^2 + \omega_c^2/4} - l\hbar\omega_c/2$, where $n = 0, 1, 2, \ldots$ is the radial quantum number, $l = 0, \pm 1, \pm 2, \ldots$ is the angular momentum quantum number, $\hbar\omega_0$ is the harmonic potential confinement energy, and $\hbar\omega_c$ is the cyclotron

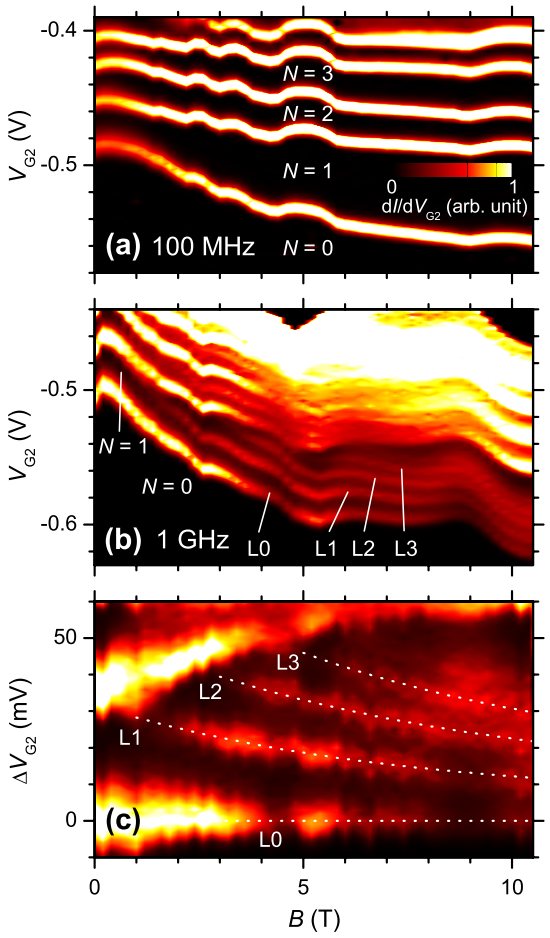

FIG. 2 (color online). (a) Behavior of the pump current in perpendicular magnetic fields B taken with $f = 100$ MHz. dI/dV_{G2} is plotted in a color scale. The regions of Nef plateaux are marked by N. (b) dI/dV_{G2} as in (a) but taken with $f = 1$ GHz. A series of additional lines ($L1$, $L2$, and $L3$) appear in the plateau regions. (c) Data in (b) replotted to show the positions of the lines $L1$, $L2$, and $L3$ on the V_{G2} axis relative to the $L0$ line. The dotted lines for $L1$, $L2$, and $L3$ show fits to Fock-Darwin states of a circular dot.

energy ($= \hbar eB/m^* \sim 1.7$ meV/T, where m^* is the effective mass of conduction-band electrons in GaAs).

The excitation lines ($L1$, $L2$, and $L3$) shown in Fig. 2(c) were fitted to a function $F(B) = \alpha[E(0, l) - E(0, 0)] = \alpha l(\hbar\sqrt{\omega_0^2 + \omega_c^2/4} - \hbar\omega_c/2)$ with $l = 1$, 2, and 3, respectively. These quantum numbers are chosen because the lowest energy Fock-Darwin states at high B are those with $n = 0$ and positive l. We used a scaling factor α to convert the energy scale to the ΔV_{G2} scale. For the best fit, we used different α and ω_0 as fitting parameters for each excitation line. The B dependence of $E(0, l) - E(0, 0)$ gives a unique curvature for a given ω_0. Therefore, even when we do not know the experimental value of α, we can estimate $\hbar\omega_0$ from the fit. The fits are shown as dotted lines in Fig. 2(c). Although our quantum dot is not expected to be perfectly circular, and the confinement potential is not necessarily parabolic, the observed excitation lines fit well to the Fock-Darwin spectrum. The fitting parameters used were $\hbar\omega_0 = 7.7 \pm 0.3$, 9.0 ± 0.4, and 8.4 ± 0.6 meV and $\alpha = 4.1 \pm 0.2$, 2.9 ± 0.2, and 3.0 ± 0.3 for $L1$, $L2$, and $L3$ lines, respectively. In our fits, α varied $\sim$30%, but $\hbar\omega_0$ was consistent at 8–9 meV, although nontrivial corrections due to nonparabolicity and asymmetry in the potential must be taken into account for a more accurate estimate. We note that similar spectra were observed in the reverse field direction and in all three samples (with slightly different designs) that we have measured, although the strength of the spectrum varied from sample to sample.

The time-dependent nature of the observed excitations becomes clearer when the pumping frequency, and hence the rate of confinement potential modulation, is varied. Figures 3(a) and 3(b) plot dI/dV_{G2} as a function of frequency taken at $B = 0$ and 6 T, respectively. At $B = 0$ T, no signature of excitation is observed even at $f = 1.6$ GHz. At $B = 6$ T, $L1$, $L2$, and $L3$ lines gradually appear as f is increased. The occupation probabilities of each state can be deduced from the current values at the miniature plateaux that appear between the excitation lines. Figure 3(c) shows the probabilities deduced from the data in Fig. 3(b). The occupation probabilities of the excited states increase almost linearly until they reach a saturation value. The ground-state occupation decreases accordingly. We believe that the saturation of excitations into a particular state is caused by further excitations into higher excited states (i.e., the electron excited into the $L1$ state is again excited into $L2$, $L3$, and so on). At the higher end of the frequency range, a population inversion occurs; the excited states become more populated than the ground state. This suggests that excitation processes such as thermal excitations, that favor ground-state occupation, are unlikely to be the origin.

The magnetic-field and frequency dependences suggest that the observed spectrum is indeed due to nonadiabatic transitions by the time-dependent potential [19]. The transition probabilities and the number of excited states involved can be tuned by the pump frequency and the external magnetic field. One noteworthy feature in our experimental data is how the excitation spectrum persists to lower frequency [as low as 100 MHz in Fig. 3(c)] at $B = 6$ T, while no signature of excitations appears at zero field. To observe the excitation lines, the excitation energy gap needs to be smaller than the energy required to retain the second electron (i.e., charging energy), so that they appear in the $N = 1$ plateau region. If this is not the case, the lines will be masked by the $N = 1$ to $N = 2$ transition [see the region $B \sim 2$ T in Figs. 2(b) and 2(c)]. However, nonadiabatic excitations may still occur in the $N = 1$ region and would result in a reduction in the plateau value. We have not observed such behavior in our experiments at $B = 0$. Nonadiabatic transition probabilities in general depend on the size of energy gap between the states, but also the nature of the wave functions is important [1]. From Fig. 2(c), the energy gap was found to differ only

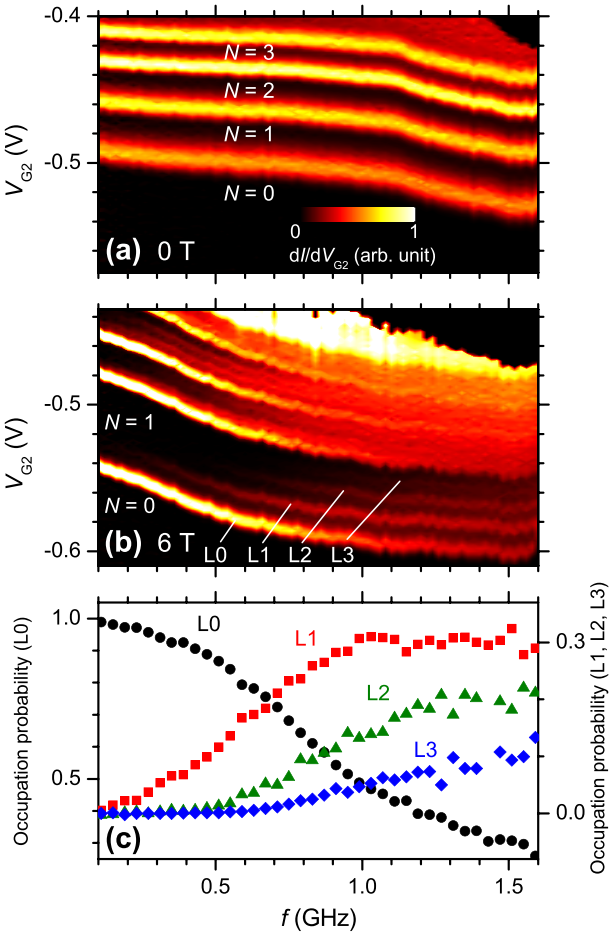

FIG. 3 (color online). (a) Frequency dependence of the pump current at zero magnetic field. dI/dV_{G2}, rescaled to take into account the effect of a frequency change on the ef value, is plotted in a color scale. (b) Frequency dependence at $B = 6$ T, showing the excitation lines $L1$, $L2$, and $L3$ gradually appearing as f increases. (c) Occupation probabilities of the ground state ($L0$) and excited states ($L1$, $L2$, and $L3$) deduced from the data in (b). The data for $L0$ are plotted against the left axis, while the rest are on the right axis.

by ~50% between 0 and 6 T. The change is not large enough to account for the enhancement of the excitation in the magnetic field. We speculate that this behavior is related to qualitative changes in the wave function in a perpendicular magnetic field. We also note that excitation lines also appear in the $N = 2$ and $N = 3$ regions [see Fig. 1(i) and Figs. 2(b) and 3(b), respectively]. These excitation lines are often stronger than the lines in the $N = 1$ region, suggesting that multiple-electron systems are more easily perturbed to cause nonadiabatic transitions.

In summary, we report the observation of a Fock-Darwin excitation spectrum in a single-electron system due to nonadiabatic modulation of the confinement potential. By observing loss of current quantization in an electron pump, we have probed for the first time the structure of electronic states in a dynamic quantum dot. We demonstrate that the transition probability can be tuned by varying the operation frequency, showing the crossover from the adiabatic to the nonadiabatic regime. This may be a mechanism that limits the high-frequency operation of the electron pumps for current standard applications [15]. Our method provides a model system to study the nature of nonadiabatic processes and may be useful in the state manipulation of single-electron dots.

We thank S. J. Wright, H.-S. Sim, A. Tzalenchuk, J. Hannay, and J. Williams for useful discussions. This work is supported by the United Kingdom Department for Business, Innovation and Skills, the European Metrology Research Program, Grant No. 217257, and the United Kingdom EPSRC.

[1] H. R. Lewis and W. B. Riesenfeld, J. Math. Phys. (N.Y.) **10**, 1458 (1969).
[2] H. Nakamura, *Nonadiabatic Transition: Concepts, Basic Theories and Applications* (World Scientific, Singapore, 2002).
[3] A. Assion *et al.*, Science **282**, 919 (1998).
[4] R. J. Levis, G. M. Menkir, and H. Rabitz, Science **292**, 709 (2001).
[5] J. R. Petta *et al.*, Science **309**, 2180 (2005).
[6] F. H. L. Koppens *et al.*, Nature (London) **442**, 766 (2006).
[7] M. Atatüre *et al.*, Science **312**, 551 (2006).
[8] J. M. Martinis *et al.*, Phys. Rev. Lett. **89**, 117901 (2002).
[9] K. B. Cooper *et al.*, Phys. Rev. Lett. **93**, 180401 (2004).
[10] C. Monroe *et al.*, Phys. Rev. Lett. **75**, 4714 (1995).
[11] C. Roos *et al.*, Phys. Rev. Lett. **83**, 4713 (1999).
[12] S. Tarucha *et al.*, Phys. Rev. Lett. **77**, 3613 (1996).
[13] L. P. Kouwenhoven *et al.*, Science **278**, 1788 (1997).
[14] M. D. Blumenthal *et al.*, Nature Phys. **3**, 343 (2007).
[15] S. P. Giblin *et al.*, New J. Phys. **12**, 073013 (2010).
[16] V. Kashcheyevs and B. Kaestner, Phys. Rev. Lett. **104**, 186805 (2010).
[17] To confirm that single-electron dots are formed, the observation of ef quantization is not enough. This is because there may be some electrons left in the dot that are not pumped out at the end of the cycle (4) in Fig. 1(c) and hence do not contribute to the pump current. If this is the case, further increasing the amplitude of barrier modulation would pump out more electrons and produce a larger current. If there is no electron left at the end of the cycle, no current increase would be observed. This test was carried out to confirm that a single-electron dot was formed during each cycle.
[18] The rf output power used was 0 dBm for the data shown in Figs. 1(f) and 1(h) and in Fig. 2(a) and 5 dBm for the data shown in Figs. 1(g) and 1(i), in Fig. 2(b) [and 2(c)], and in Fig. 3. The 0 dBm output corresponds to the ~600 mV peak to peak amplitude of gate voltage oscillations.
[19] The ~1 GHz pump frequency may seem too small to excite nonadiabatic transitions across an energy gap of the order of meV. However, it is not the overall frequency that determines the nonadiabatic transition probability but the rate of parameter change. We estimate the rate of barrier change to be at least a few mV per 10 ps, which may be large enough to cause nonadiabatic excitations.